Available online at BCREC Website: http://bcrec.undip.ac.id

Bulletin of Chemical Reaction Engineering & Catalysis, 12 (3), 2017, 460-468

Research Article

Nano-Magnetic Catalyst CaO-Fe_3O_4 for Biodiesel Production from Date Palm Seed Oil

Mortadha A. Ali[1*], Imad A. Al-Hydary[2], Tahseen A. Al-Hattab[1]

[1]*Department of Electrochemical Engineering, College of Engineering, University of Babylon, Hilla City, Iraq*

[2]*Department of Ceramics and Building Materials, College of Materials Engineering, University of Babylon, Hilla City, Iraq*

Received: 25th January 2017; Revised: 11st July 2017; Accepted: 12nd July 2017; Available online: 27th October 2017; Published regularly: December 2017

Abstract

A nanocatalyst of CaO supported by Fe_3O_4 magnetic particles was prepared by a chemical precipitation method. It was characterized by various techniques including X-ray diffraction, transmission electron microscopy (TEM), scanning electron microscopy (SEM); Fourier transforms infrared spectroscopy (FTIR), and Hammett indicator. It has been found that the catalyst consists of CaO and Fe_3O_4 accompanied by $CaFe_2O_4$. This composite catalyst was used for the catalytic transesterification of palm seed oil. The results revealed that the highest biodiesel yields for palm seed oil of 69.7% can be obtained under the conditions of (65 °C reaction temperature, 300 min reaction time, 20 methanol/oil molar ratio, and 10 wt.% of CaO/Fe_3O_4 catalyst loading). The physicochemical properties of the biodiesel produced from palm seed oil were further studied and compared with the ASTM and the EN biodiesel specifications. The results showed that the properties of the biodiesel produced comply with the international standard specifications.

Keywords: Biodiesel; Nano-magnetic catalyst; Transesterification; Metal oxide; Palm seed oil

How to Cite: Ali, M.A., Al-Hydary, I.A., Al-Hattab, T.A. (2017). Nano-Magnetic Catalyst CaO-Fe_3O_4 for Biodiesel Production from Date Palm Seed Oil. *Bulletin of Chemical Reaction Engineering & Catalysis*, 12 (3): 460-468 (doi:10.9767/bcrec.12.3.923.460-468)

Permalink/DOI: https://doi.org/10.9767/bcrec.12.3.923.460-468

1. Introduction

Since the invention of the diesel engine massive amounts of diesel fuel, derived from fossil oil, had been used. Aside from the environmental issues related to the extraction and refining of the crude oil to get the diesel fuel, the diminishing of the petroleum reserves urges the researchers to find new renewable and sustainable sources for the diesel [1]. Over the last years biodiesel has become new energy source that have great importance [2]. The name "biodiesels" has been given to transesterified-vegetable oils to describe their use as diesel fuel [3]. In addition to being fully competitive to petroleum diesel in most technical aspects; biodiesel has become more attractive because of several distinctive advantages. It is renewable, nonhazardous, biodegradable, and has low emission profiles, so it is environmentally serviceable [4].

The homogeneous base catalyzed transesterification method is the conventional production method of the biodiesel from vegetable oils. This method utilizes potassium hydroxide or sodium

* Corresponding Author.
E-mail: mortada89_1989@yahoo.co.uk (M.A. Ali)
Telp.: +9647706087028

hydroxide as homogenous base catalyst to produce the biodiesel at very high yield under moderate conditions [5]. However, the inability to reuse the homogenous catalyst, the use of the chemicals for its neutralization, and the high amount of wastewater produced by its removal processes are the main drawbacks facing the conventional method. Therefore, the use of such production method addresses environmental and cost issues that hinder the commercialization of biodiesel [6,7].

Numerous researches have been conducted to replace the homogenous catalyst by suitable heterogeneous catalyst. The later should have strong basic sites and durable activity. It also must be environmental-friendly and easily to recover and reuse [8-10]. Many research works showed that CaO has great potential to be used as heterogeneous catalyst in transesterification of vegetable oils [11]. However, the separation of CaO from the products of the reaction and its reuse still considerable unsolved issues especially when the CaO nanoparticles are used [12]. Despite the higher activity of nanocatalyst, the difficulty of separation is high.

The magnetic catalysts have the advantage over the non-magnetic catalysts in the separation process. As compared with the filtration or centrifugation processes, the use of magnetic separation process can avoid the loss of catalyst and increase its reusability [13,14]. Different types of ferrites have been used as magnetic catalyst [10] or catalyst support [12].

In the current work, nano-magnetic heterogeneous base catalyst has been developed. It consists of CaO nanocatalyst supported by Fe_3O_4 magnetic particles. Palm seeds oil, which is extracted from the seeds of Iraqi date palm (Phoenix Dactylifera), was used to evaluate the catalytic activity of the catalyst in transesterification reaction. The effect of reaction temperature and catalyst content were investigated.

2. Materials and Method

2.1 Materials

The date palm fruits of Phoenix Dactylifera were collected from farmlands in Karbala city in the south of Iraq. Magnetic ferrite powder (Fe_3O_4>99%) was purchased from Hongwu International Group. Calcium nitrate ($Ca(NO_3)_2.4H_2O$, 99%, Fluka), neutral red (Fluka), 2,4-dinitroaniline (Fluke), Sodium hydroxide (96%, BDH Industries), N-hexane (97%,Sinopharm Chemical Reagent Co.), Methanol (99.9%, Scharlab), Phenolphthalein (Loba Chemie Pvt.), and Bromothymol blue (Loba Chemie Pvt.) were analytical reagents and were used as received without further purification.

2.2 Oil extraction from date palm seeds

The date palm seeds were separated manually from the fruits and washed with distilled water to remove the peels. They were dried under the sun and grinded using a mechanical grinder (RRH-A500). N-hexane, as a solvent, and soxhlet apparatus were used to extract the oil from the grinded seeds. The extracted oil was separated from n-hexane by rotary evaporator (Stuart, England) under vacuum conditions.

2.3 Preparation of nano-magnetic catalyst

In the current work, it was desired to prepare CaO nanocatalyst supported by Fe_3O_4 magnetic particles. For this purpose, 0.003 M calcium nitrate solution was prepared by dissolving an appropriate amount of calcium nitrate in deionized water. The 3.5 g of Fe_3O_4 were added to 5 L of the solution. The mixture was firstly mixed by mechanical stirrer for five minutes at 1500 rpm and then put in an ultrasonic bath (SB 5200 DTD) for 15 minute to get a well dispersed suspension. Sodium hydroxide solution (2 M) was added drop by drop to the suspension, which was under stirring at 1500 rpm, until the pH of 12 was obtained. The suspension was aged overnight under stirring at the same speed. The precipitate was washed by deionized water and centrifugation until the pH around seven was obtained. It was dried overnight in oven at 80 °C.

The product was grinded by mortar and pistil and calcined at 550 °C for one hour in an electric box furnace. The catalyst was kept in a bowl containing silica gel to reduce the risk of contamination by atmospheric CO_2 and moisture.

2.4 Characterization of nanomagnetic catalyst

The powder X-ray diffraction analysis (XRD) was employed to identify the crystalline structure of nanomagnetic catalyst CaO-Fe_3O_4. The analysis was performed on a Shimadzu model XRD 6000 Power X-ray diffractometer using Cu-Kα radiation (40 kV and 30 mA) with wavelength (λ) of 1.5406 Å. Data were collected over a 2θ range from 20° to 70° with a step of 0.02° at speed 6 degree/minute. Diffraction peaks of the crystalline phases were matched with those of standard compounds described in the JCPDS (Joint Committee on the

Powder Diffraction Standards) databank. The transmission electron microscope (Zeiss-EM10C-80 Kv) and scanning electron microscope (TESCAN, Chic Slovakia) were used to investigate the morphology, the size, and the aggregation of the catalyst particles. FTIR technique was used to inspect the chemical transformation of catalysts using FTIR-8300 spectrometer (Bruker, Germany).

Hammett indicator procedure was followed to determine the basic strength (H–) and basicity of the synthesized catalyst. The basicity is the number of basic sites found on the catalyst surface. Basic strength of a solid base is the ability of the surface to accept a proton or donates an electron pair. It determines the activity of the catalyst. The Hammett indicators used in this work are given in Table 1.

The procedure involved the dilution of 1 mL of Hammett indicator with 10 mL of methanol. 300 mg of catalyst was added to the solution and was left for two hours to reach an equilibrium state where no additional change of color took place. The change in the color of the solution was used to indicate the strength of the catalyst. The base strength is quoted as being stronger than the weakest indicator which exhibits a colour change, but weaker than the strongest indicator that produces no change. The basicity value (mmol/g) of the catalyst was determined using Hammett indicator-benzene carboxylic acid (0.02 mol/L anhydrous ethanol solution) titration method. After two hours of the addition of the catalyst to the indicator solution, the benzene carboxylic acid was added until the colour of solution changes back to the original colour before adding the catalyst.

2.5 Transesterification reaction

Batch reactor was used for transesterification of palm seeds oil to produce biodiesel. The reactor was 100 mL glass round bottom flask with three necks equipped with a reflux condenser and thermocouple. Ten grams of palm seed oil were preheated to desired temperature by hot plate magnetic stirrer then the desired amount of catalyst was added. After adding the catalyst, 8.34 g of anhydrous methanol was added to the base of the reactor to prevent the evaporation of methanol (methanol/oil molar ratio ≈ 20:1). It has been assumed that the point of adding the methanol represent the starting point of reaction. The agitation speed was kept constant at 400 rpm; also the reaction time was fixed at five hours for all experiments. After reaction, the products were separated by centrifuge (Ultra-8V, Chain) at speed of 3000 rpm for 15 min. They were separated into three layers. The top layer consist of biodiesel and methanol. The middle layer is glycerol and unreacted oil. The bottom layer is catalyst. The biodiesel yield was calculated using Equation (1) [6,15-18].

$$Yield\ (\%) = (Weight\ of\ biodiesel\ (FAME) / Weight\ of\ oil) \times 100\% \quad (1)$$

The effect of the following parameters on the transesterification reaction were investigated: (1) the amount of the catalyst loading in reactor (1%, 5%, and 10% based on oil weight); (2) the reaction temperature (45 °C, 55 °C, 65 °C).

Table 1. Hammett indicators used to determine the basic strength

Indicators name	Basic strength (H–)	Color change
Neutral red	6.8	Red to yellow
Bromothymol blue	7.2	Yellow to blue
Phenolphthalein	9.8	Colorless to red
2, 4-dinitroaniline	15.0	Yellow to violet

2.6 Properties of date seed biodiesel

The fatty acid methyl esters of biodiesel were analyzed using Gas Chromatography-Mass spectrometry (GC-MS)Agilent 7890A GC series (Hewlett Packard, USA) with flame ionization detector (FID) and HP column, 30 m long × 0.32 mm ID × 0.25 µm film thickness (SGE, Australia). An amount of 0.2 mL of the prepared biodiesel was added to 1 mL of hexane and 2-propanol with volume ratio of (4/5). After filteration through 0.2 µm polytetrafluoroethylene syringe micro filter, 1-µL of the sample was manually injected into the GC/MS using a 5-µL micro syringe (SGE, Australia). The GC/MS instrument conditions are given in Table 2. Density and kinematic viscosity of biodiesel was predicated by using Cone-Plate test (DV-III ultra) and four digital high precision density tester, respectively. Saponification value (SV) and iodine value (IV) of oil were calculated from fatty acid compositions of oil with the help of Equations (2) and (3), respectively [19]:

$$SV = \frac{\Sigma\,(560 \times Ai)}{MWi} \quad (2)$$

$$IV = \frac{\Sigma\,(254 \times D \times Ai)}{MWi} \quad (3)$$

where MW_i is the molecular weight of each component, A_i is the percentage of each fatty acid, and D is the number of double bonds .

Higher heating value (HHV), Cetane number (CN) and Flash point (FP) of biodiesel were calculated from Equations (4), (5) [19], and (6) [3], respectively, where V is the viscosity in cSt.

$$HHV = 49.43 - [0.041(SV) + 0.015(IV)] \quad (4)$$
$$CN = 46.3 + (5458/SV - 0.225 \times IV) \quad (5)$$
$$FP = 32.641V + 305.02 \quad (6)$$

3. Results and Discussion

3.1 Characterization of nanomagnetic solid catalyst

Figure 1 shows photograph image of the prepared CaO-Fe_3O_4 catalyst. It shows the response of the catalyst to the magnet confirming that it is ferromagnetic material. It can be seen that the color of CaO/Fe_3O_4 catalyst changes from black to brown-red after calcination at 550 °C for 1 h.

3.1.1 Results of XRD test

Figure 2 shows the XRD patterns of the nanomagnetic catalyst after calcination at 550 °C for 1 h. The observed positions of the diffraction lines (2θ and corresponding $d_{2\theta}$) for the pattern are in full agreement with the corresponding values reported for calcium oxide (JCPDS, Card No. 028-0775), calcium ferrate (JCPDS, Card No. 032-0168), and magnetite (JCPDS, Card No.13-534). This indicates that the change of the color, after calcination, is due to the formation of calcium ferrate.

Table 2. Operating conditions for the GC/MS

Parameters	Value
GC	
Carrier gas	Helium
Operation mode	Constant flow
Inlet temperature (°C)	250
Oven temperature (°C)	240
Injection volume (µl)	1
Split ratio	1:50
Run time (min)	20
Average velocity (cm/sec)	37.789
Pressure (psi)	17.04
MS	
Transfer line temperature (°C)	240
Source temperature (°C)	220
Solvent delay (min)	2
Scan mass range	450-500

3.1.2 Results of FTIR test

The FTIR spectra of the nano-magnetic catalyst CaO-Fe_3O_4 before and after the calcination are shown in Figure 3. The IR absorption peaks observed at 554 cm^{-1} are corresponding to the Fe–O stretching vibration of the Fe_3O_4. The band at 2360 cm^{-1} corresponds to the presence of atmospheric CO_2 whereas the band at 678 cm^{-1} is due to water release. The broad band at 1369 cm^{-1} and sharp band at 865 cm^{-1} correspond to CO_3^{-2} in $CaCO_3$ [20-23]. After calcination, the intensity of these peaks

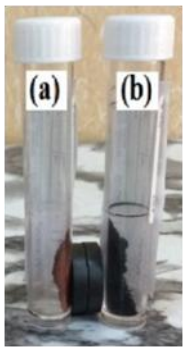

Figure 1. Photograph of nanomagnetic catalyst (a) CaO-Fe_3O_4 after calcination; (b) CaO-Fe_3O_4 before calcination

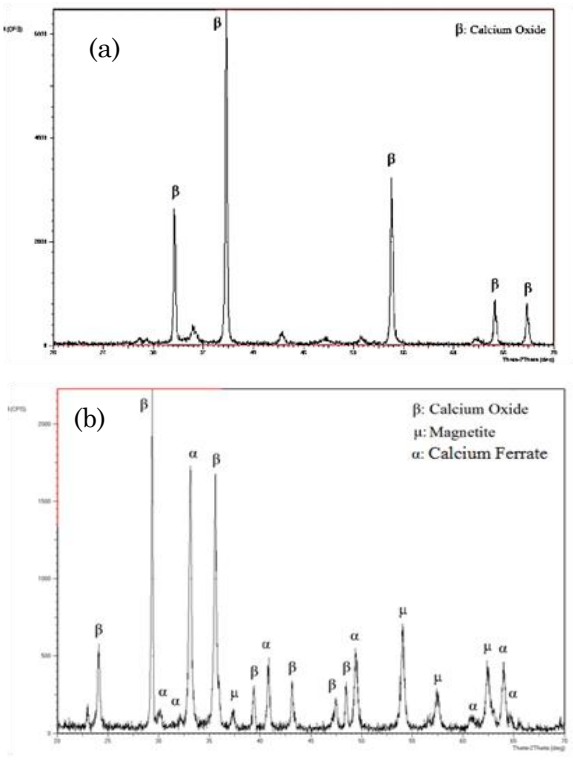

Figure 2. The XRD patterns of the (a) nano CaO (before calcination); (b) nano CaO/Fe_3O_4 (after calcination) at 550 °C for 1 h

was decreased. In addition, a new peak appeared at 441 cm^{-1}. This peak represents Fe–O band for different components of iron which may belongs to the formed calcium ferrate [23].

3.1.3 SEM and EDX analysis

The SEM images of the Fe_3O_4 particles before the deposition of CaO are shown in Figure 4. The image at low magnification shows that the powder has narrow particle size distribution, while the image at high magnification shows that the powder consists of submicron multifaceted particles. Figure 5 shows the SEM images of the prepared CaO-Fe_3O_4 catalyst after calcination. Comparing these images reveals that no significant differences can be observed, before and after calcination, except the coarsening of some Fe_3O_4 particles due to the heat treatment. This suggests a good dispersion of CaO on the surface of Fe_3O_4.

The EDX spectrum and the weight percent of the prepared catalyst are shown in Figure 6. EDX spectrum demonstrates that the surface of the catalyst had Ca/Fe/O molar ratio of (1.00/2.16/10.36) indicating, with the help of XRD results, that the surface is mainly composed of $CaFe_2O_4$ and CaO. The high molar ratio of oxygen might be due to gases adsorbed on the surface of catalyst.

3.1.4 Results of TEM test

Figure 7 shows the transmission electron microscope image for the prepared nano-magnetic catalyst. It confirms the formation of aggregates of nanoparticles, representing the deposited catalyst, that partially cover the magnetite particles. Based on the XRD results, the deposited nanocatalyst is consisting of calcium oxide and calcium ferrate.

3.1.5 Results of basicity measurement

The basic strength of the nanocatalyst supported on magnetite is 9 < H_< 15, however, the basicity of the catalyst, i.e. the number of basic sites of a certain strength, corresponds to 0.133 mmol/g of basic sites having the strength of H=9.

3.2 Activity of catalysts

3.2.1 The effect of amount of catalyst

The effect of the weight percent of the catalyst on the yield of biodiesel is shown in Figure 8. As expected, it has been observed that the yield of biodiesel increases when the weight percent of the catalyst increases. This is due to the increase of the available surface area of the catalyst per unit volume of the reaction media, and hence, the increase of the basic sites required for the catalytic reaction [24].

3.2.2 The effect of reaction temperature

Figure 8 shows the effect of the reaction temperature on the yield of biodiesel. In general, the rate of the reaction is directly proportional to the reaction temperature. The in-

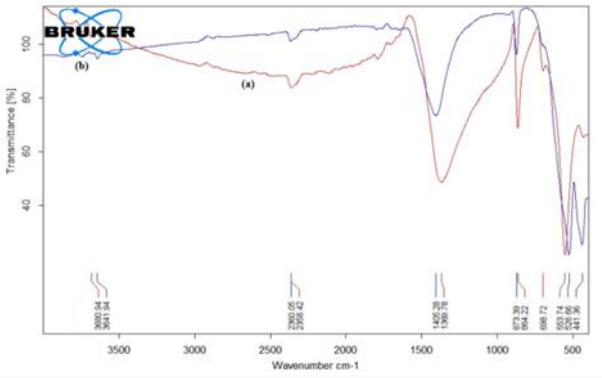

Figure 3. The FTIR spectra of the nano-magnetic catalyst CaO-Fe_3O_4 (a) before calcination; (b) after calcination at 550 °C for 1 h

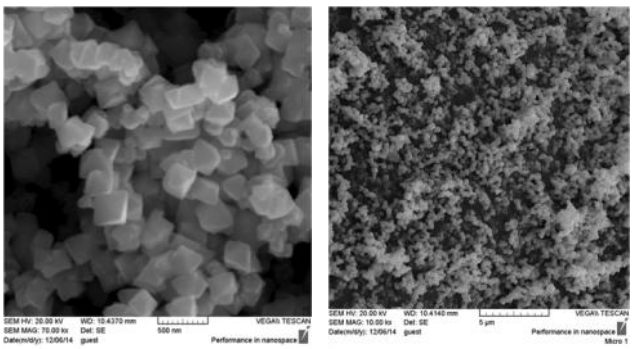

Figure 4. SEM images of Fe_3O_4 before the deposition of CaO

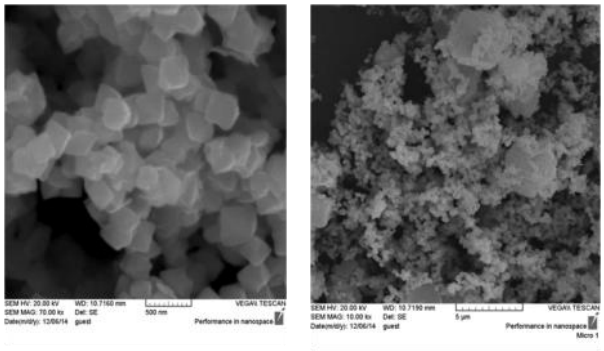

Figure 5. SEM images of the nano-magnetic catalyst CaO-Fe_3O_4 calcined at 550 °C for 1h

creasing of the temperature reduces the mass transfer limitations due to decrease in the viscosity of the reactants. This allows more particles to collide due to the increase in the energy supplied to the system. Moreover, temperature rising may reduce the amount of the absorbed gases on the surface of the catalyst, as noticed by EDX test, and hence, the available sites of reaction will eventually increase.

It has been observed that the weight percent of the catalyst has more influence on the yield of biodiesel than the reaction temperature. The effect of temperature at low weight percents is weaker than that at high weight percent of catalyst. This is possibly because the transesterification is a catalytic reaction and goes faster when the basic sites and the contact surface area for reaction increase [25,26].

3.3 Characterization of biodiesel

3.3.1 Gas chromatography analysis

GC analysis was used to diagnose the numerous composites in the produced biodiesel. Fatty acid compositions of the palm seeds oil (PSO) methyl ester detected through the study are listed in the Table 3 and the GC chromatogram is depicted in Figure 9. The results showed that the oleic acid had the highest amount among unsaturated fatty acid while palmitate acid had the highest amount among saturated fatty acid.

3.3.2 Physicochemical properties of the synthesized biodiesel

Table 4 represents some properties of biodiesel which is produced from transesterifica-

Table 3. The fatty acid compositions of the palm seed oil

Retention time (min)	Identified compounds	Saturation	Weight (%)
1.773	Caprlyic acid	C8:0	0.7
1.9	Capric acid	C10:0	0.713
2.13	Lauric acid	C12:0	11.363
2.311	Tridecanoic acid	C13:0	0.103
2.557	Myristic acid	C14:0	11.447
2.883	Pentadecenoic acid	C15:0	0.068
3.338	Palmitate acid	C16:0	13.848
3.922	Heptadecanoic acid	C17:0	0.14
4.613	Oleic acid	C18:1	51.456
4.766	Stearate acid	C18:0	6.56
6.886	Cis-11 eicosenoic acid	C20:1	1.297
7.224	Eicesnoic acid	C20:0	1.175
11.691	Heneicosanoic	C22:0	0.75
19.620	Lignocerate acid	C24:0	0.397

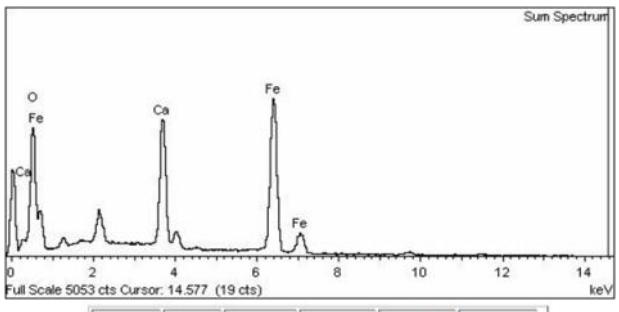

Element	App Conc.	Intensity Corrn.	Weight%	Weight% Sigma	Atomic%
O K	176.72	0.5622	50.78	0.50	76.63
Ca K	75.24	0.9906	12.27	0.18	7.39
Fe K	194.71	0.8512	36.95	0.42	15.98
Totals			100.00		

Figure 6. EDX spectra of the nano-magnetic catalyst CaO-Fe_3O_4 calcined at 550 °C for 1 h

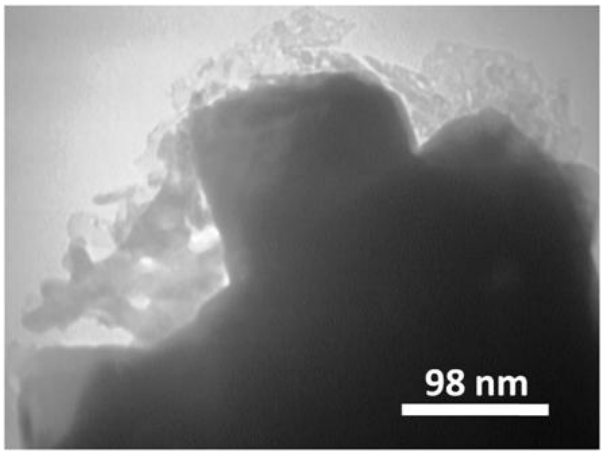

Figure 7. TEM image of nano-magnetic catalyst CaO-Fe_3O_4 calcined at 550 °C for 1 h

tion of palm seeds oil compared with biodiesel produced from other sources. The high cetane number of biodiesel return to the presence of saturated compounds in chemical composition of biodiesel where cetane number (CN) is based on two compounds, hexadecane (methyl palmitate), with a CN of 100, and heptamethylnonane, with a CN of 15 [3]. High cetane number, low viscosity and low flash point are the main advantages of date seed biodiesel. Because of these factors, the palm seed biodiesel is preferred than the other biodiesel fuels as it can increase engine's output and decrease pollution. These results are comparable with those obtained by Amani *et al*. [19]. These findings are inconsistent with the typical range of ASTM and EN.

3.3.3 Results of FTIR test

Figure 10 shows the FT-IR spectra of the biodiesel. It is similar to the FT-IR spectra of the palm seeds oil (PSO), given in Figure 11, because of the analogous in the chemical natures of the oil and FAME. Nevertheless, slight dissimilarities were noticed. The peaks emerged at 1743, 1376, 1157, and 852 cm^{-1} in the PSO were moved to 1741, 1361, 1169, and

Table 4. Characteristics of date palm seed biodiesel in comparison with the other biodiesel fuel

Characteristics	V_s (mm^2/s)	D_n (g/cm^3)	*CN*	*HHV* (kJ/g)	*FP* (°C)	References
Date Seed	3.95	0.885	62.67	40.309	160	Current study
Date Seed	3.84	0.877	60.3	39.55	140	[19]
Palm	5.7	0.88	60	--	--	[19]
Coconut	--	--	65.3	38.67	--	[19]
ASTM (B100)	1.9 -6	--	64.7	--	130	[27]

V_s, viscosity; D_n, density; CN, cetane number; HHV, higher heating value; FP, flash point

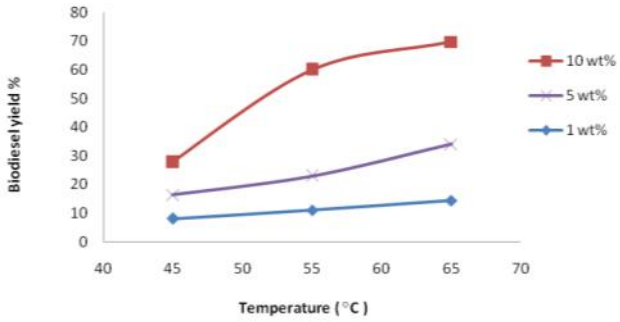

Figure 8. The effect of reaction temperature and weight percent of catalyst on biodiesel yield at reaction time of 5 h, methanol/oil ratio: 20/1 and agitator speed of 400 rpm

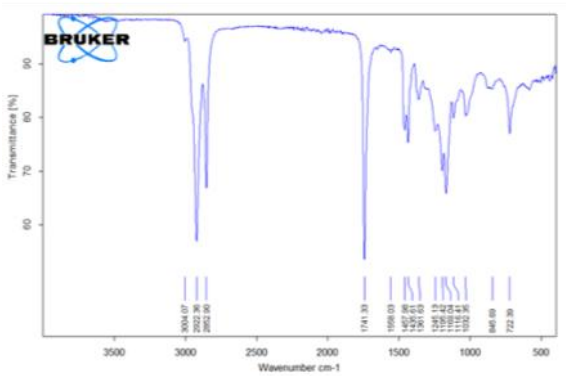

Figure 10. The FTIR spectra of the palm seeds oil methyl ester

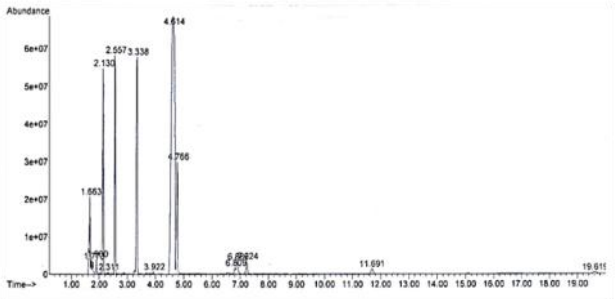

Figure 9. GC/MS diagram of palm seeds oil methyl ester

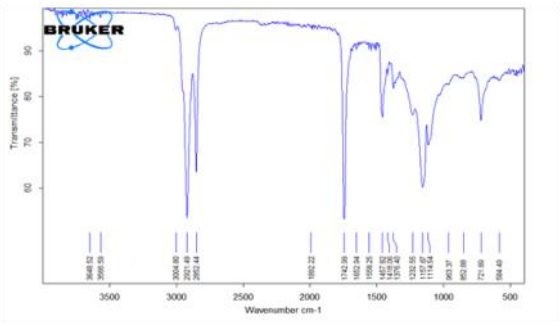

Figure 11. The FTIR spectra of palm seeds oil

845 cm^{-1} in the FAME, respectively. So, the demise of the peaks at 1418 and 963 cm^{-1} from the spectra of the PSO and outcrop of new peaks in the biodiesel at 1435 cm^{-1} and 1195 cm^{-1} clearly illustrate the transmutation of PSO into FAME. Furthermore, the disappearance of the peak at 3500 cm^{-1} region, referred to the O–H bonds of the water molecule, proposes that produced FAME has low water content [6].

4. Conclusions

Heterogeneous base nanocatalyst of CaO-Fe_3O_4 based on Fe_3O_4 magnetic core was prepared by chemical precipitation method. Different techniques were used to characterize the catalyst. The consequences showed that the prepared catalyst consist of agglomerates of CaO nanocatalyst supported by the magnetite particles and their composite have ferromagnetic properties. The formation of this composite magnetic catalyst accompanied by the formation of $CaFe_2O_4$. A maximum biodiesel yields of 69.7% was obtained under the conditions of (65 °C reaction temperature, 300min reaction time, 20/1 methanol/oil molar ratio and 10 wt.% of CaO/Fe_3O_4 catalyst amount).

It was found that the catalyst amount and time had the most significant influence on biodiesel yields, while the impact of reaction temperature was not significant at low amount of catalyst. The nanomagnetic solid base catalyst, CaO/Fe_3O_4, used in the preparation of biodiesel illustrate a good prospect of development and application. The most important advantages of date seed biodiesel are its high cetane number, low viscosity and flash point. These factors can increase engine's output and decrease pollution in comparison with other biodiesel fuels. The present experimental results support that methyl ester of date seed oil can be successfully used as biodiesel in the internal combustion engine.

Acknowledgements

The collaboration of Electrochemical Engineering Department staff at University of Babylon in this project is gratefully acknowledged.

References

[1] Maceiras, R., Vega, M., Costa, C., Ramos, P., Márquez, M.C. (2009). Effect of methanol content on enzymatic production of biodiesel from waste frying oil. *Fuel*, 88: 2130-2134.

[2] Zhanga, Y., Dubé, M.A., McLean, D.D., Kates, M. (2003). Biodiesel production from waste cooking oil: Economic assessment and sensitivity analysis. *Bioresource Technology*, 90: 229-240.

[3] Demirbas, A. (2008). *Biodiesel: a realistic fuel alternative for diesel engines*. Springer. London.

[4] Ma, F., Hanna, M.A. (1999): Biodiesel production: a review. *Bioresource Technology*, 70: 1-15.

[5] Semwal, S., Arora, A.K., Badoni R.P., Tuli, D.K. (2011). Biodiesel production using heterogeneous catalysts. *Bioresource Technology*, 102: 2151-2161.

[6] Farooq, M., Ramli, A., Subbarao, D. (2013). Biodiesel production from waste cooking oil using bifunctional heterogeneous solid catalysts. *Journal of Cleaner Production*, 59: 131-140.

[7] Endalew, A.K., Kiros, Y., Zanzi, R. (2011). Heterogeneous catalysis for biodiesel production from Jatropha curcas oil (JCO). *Energy*, 36: 2693-2700.

[8] Kafuku, G., Mbarawa, M. (2010). Alkaline catalyzed biodiesel production from moringa oleifera oil with optimized production parameters. *Applied Energy*, 87: 2561-2565.

[9] Gao, L., Teng, G., Lv, J., Xiao, G. (2010). Biodiesel synthesis catalyzed by the KF/Ca-Mg-Al hydrotalcite base catalyst. *Energy Fuels*, 24: 646-651.

[10] Xue, B., Luo, J., Zhang, F., Fang, Z. (2014). Biodiesel production from soybean and Jatropha oils by magnetic $CaFe_2O_4$-$Ca_2Fe_2O_5$-based catalyst. *Energy*, 68: 584-591.

[11] Kouzu, M., Kasuno, T., Tajika, M., Sugimoto, Y., Yamanaka, S., Hidaka, J. (2008). Calcium oxides a solid base catalyst for transesterification of soybean oil and its application to biodiesel production. *Fuel*, 87: 2798-2806.

[12] Hu, S., Guan, Y., Wang, Y., Han, H. (2011). Nano-magnetic catalyst KF/CaO-Fe_3O_4 for biodiesel production. *Applied Energy*, 88: 2685-2690.

[13] Ying, M., Chen, G. (2007). Study on the production of biodiesel by magnetic cell biocatalyst based on lipase-producing Bacillus subtilis. *Applied Biochemistry and Biotechnology*: 137: 793-803.

[14] Xie, W., Ma, N. (2009).Immobilized lipase on Fe_3O_4 nanoparticles as biocatalyst for biodiesel production. *Energy & Fuels*, 23: 1347-1353.

[15] Taufiq-Yap, Y.H., Teo, S.H., Rashid, U., Islam, A., Hussein, M.Z., Lee, K.T. (2014). Transesterification of Jatropha curcas crude oil to biodiesel on calcium lanthanum mixed

oxide catalyst: Effect of stoichiometric composition. *Energy Conversion and Management*, 88: 1290-1296.

[16] Charoenchaitrakool, M., Thienmethangkoon, J. (2011). Statistical optimization for biodiesel production from waste frying oil through two-step catalyzed process. *Fuel Processing Technology*, 92: 112-118.

[17] Tariq, M., Ali, S., Ahmad, F., Ahmad, M., Zafar, M., Khalid, N., Khan, M.A. (2011). Identification, FT-IR, NMR (^{1}H and ^{13}C) and GC/MS studies of fatty acid methyl esters in biodiesel from rocket seed oil. *Fuel Processing Technology*, 92: 336-341.

[18] Birla, A., Singh, B., Upadhyay, S.N., Sharma, Y.C. (2012). Kinetics studies of synthesis of biodiesel from waste frying oil using a heterogeneous catalyst derived from snail shell. *Bioresource Technology*, 106: 95-100.

[19] Amani, M.A., Davoudi, M.S., Tahvildari, K., Nabavi, S.M., Davoudi, M.S. (2013). Biodiesel production from Phoenix dactylifera as a new feedstock. *Industrial Crops and Products*, 43: 40-43.

[20] Tran, D., Chen, C., Chang, J. (2012). Immobilization of Burkholderia sp. lipase on a ferric silica nanocomposite for biodiesel production. *Biotechnology*, 158: 112- 119.

[21] Yu, C., Huang, L., Kuan, I., Lee, S. (2013). Optimized Production of Biodiesel from Waste Cooking Oil by Lipase Immobilized on Magnetic Nanoparticles. *International Journal of Molecular Sciences*,14: 24074-24086.

[22] Jacyna-Onyszkiewicz, I., Grunwald-Wyspianska, M., Kaczmarek, W. (1997). IR Studies of the Phase Transformation of Fe_2O_3 to Fe_3O_4 by Magnetomechanical Activation. *Journal de Physique IV*: 7, 615- 616.

[23] Shu, Z., Wang, S. (2009). Synthesis and Characterization of Magnetic Nanosized Fe_3O_4/MnO_2 Composite Particles. *Journal of Nanomaterials*, 10: 1-6.

[24] Buchori, L., Istadi, I., Purwanto, P. (2017). Effects of Weight Hourly Space Velocity and Catalyst Diameter on Performance of Hybrid Catalytic-Plasma Reactor for Biodiesel Synthesis over Sulphated Zinc Oxide Acid Catalyst. *Bulletin of Chemical Reaction Engineering & Catalysis*, 12 (2): 227-234.

[25] Hsiao, M., Lin, C., Chang, Y. (2011). Microwave irradiation-assisted transesterification of soybean oil to biodiesel catalyzed by nanopowder calcium oxide. *Fuel*, 90: 1963-1967.

[26] Sohpal, V.K., Singh, A., Dey, A. (2011). Fuzzy Modeling to Evaluate the Effect of Temperature on Batch Transesterification of Jatropha Curcas for Biodiesel Production. *Bulletin of Chemical Reaction Engineering & Catalysis*, 6(1): 31-38.

[27] ASTM D6751. Standard Specification for Biodiesel Fuel Blend Stock (B100) for Middle Distillate Fuels.